Research Square

Preprints are preliminary reports that have not undergone peer review.
They should not be considered conclusive, used to inform clinical practice,
or referenced by the media as validated information.

Addressing China's Wind Power Underperformance

Haiyang Lin

haiyanglin@g.harvard.edu

Harvard University https://orcid.org/0000-0003-2115-3914

Zheng Wang

Beijing Normal University https://orcid.org/0000-0003-4873-505X

Haiyang Jiang

Tsinghua University

Qie Sun

Shandong University

Jing Cao

Tsinghua University

Yang Wang

China Meteorological Administration

Chris Nielsen

Harvard University https://orcid.org/0000-0001-8043-2409

Chen Xiang

Shanghai Jiao Tong University

Michael McElroy

Harvard University https://orcid.org/0000-0002-1354-167X

Article

Keywords:

Posted Date: November 10th, 2026

DOI: https://doi.org/10.21203/rs.3.rs-11559125/v1

License: This work is licensed under a Creative Commons Attribution 4.0 International License.
Read Full License

Additional Declarations: There is **NO** Competing Interest.

Addressing China's Wind Power Underperformance

Haiyang Lin[1#]*, Zheng Wang[2#], Haiyang Jiang[1,3], Qie Sun[4,5], Jing Cao[6,7], Yang Wang[8], Chris P. Nielsen[1], Chen Xiang[9]*, Michael B. McElroy[1,10]

[1]Harvard-China Project on Energy, Economy and Environment, John A. Paulson School of Engineering and Applied Sciences, Harvard University, Cambridge, MA 02138, USA.
[2]Bay Area International Business School, Beijing Normal University, Zhuhai, 519087, China.
[3]Department of Electrical Engineering, Tsinghua University, Beijing, 100084, China.
[4]Institute of Thermal Science and Technology, Shandong University, Jinan 250061, China.
[5]Institute for Advanced Science and Technology, Shandong University, Jinan 250061, China.
[6]School of Economics and Management, Tsinghua University, Beijing 100084, China.
[7]Hang Lung Center for Real Estate, Tsinghua University, Beijing 100084, China.
[8]China Meteorological Administration Key Laboratory for Climate Prediction Studies, National Climate Centre, Beijing 100081, China.
[9]School of International and Public Affairs, Shanghai Jiao Tong University, Shanghai 200030, China.
[10]Department of Earth and Planetary Sciences, Harvard University, Cambridge, MA 02138, USA.

[#]These authors contributed equally to this work

*Correspondence to: haiyanglin@g.harvard.edu (H.L.); chen.xiang@sjtu.edu.cn (C.X.)

Abstract

Wind power is pivotal to global decarbonization, and China leads in both installed capacity and recent expansion. Yet rapid capacity expansion has not translated into commensurate growth in usable electricity. Here we reconstruct generation for 10,032 wind farms in China spanning 1989-2022 and find that over 20% of technically available generation is not utilized. Decomposition reveals that while grid-connection delays and officially reported curtailment have declined by ~70% in the past decade, a residual component - soft curtailment - has emerged. This component represents unreported losses arising from system inflexibility and regulatory distortions, such as rigid dispatch, strict curtailment targets, and premature reporting of grid connection incentivized by feed-in tariff policies. Soft curtailment now dominates wind power underperformance in China, offsetting technological improvements expected to raise capacity factors by ~20%, leaving them largely unchanged overall. Absorbing the unrealized generation through storage at multiple timescales and matching to flexible loads could enable China to reach its 2060 wind generation target for carbon neutrality up to 13 years earlier and avoid over 20 Gt CO_2 emissions cumulatively.

Introduction

China's wind power has expanded at an unprecedented pace, reaching a grid-connected capacity of 640 GW by 2025, accounting for about 50% of the world total (*1*). Yet behind this impressive scale lies a significant challenge: China's reported average wind power capacity factor (CF, the ratio of actual generation to potential generation at nameplate capacity) trails that of other nations. Wind resource assessments suggest that China and the United States share similar theoretical CFs (*2*). However, China's wind generation did not surpass that of the United States until 2016, when its installed capacity was approximately twice as large (*3*). Beyond national averages, this mismatch of expectations and reality also holds at regional level. Inner Mongolia, for example, hosts China's largest wind installation and often projected to achieve CFs of 35-60% (*4-6*), yet it recorded only 25.9% in 2023, well below Yunnan's nation-leading 32.4% (*7*). These contrasts highlight the significant gap between expected and realized (i.e., actually dispatched) wind power generation in China.

Understanding this persistent gap is critical for advancing China's carbon neutrality goals. Early studies by Lu et al. (*2*) and Huenteler et al. (*8*) examined the pre-2013 period, attributing underperformance to delayed grid connection, turbine quality issues, and high levels of curtailment. Since then, however, China's wind sector has undergone profound transformation. Installed capacity has expanded more than fourfold with the deployment of advanced turbines and offshore expansion, while reported curtailment rates have fallen sharply from 10.7% in 2013 to 2.7% in 2023 (*7*). Despite these advances, national wind CF has only increased from 23.7% to 25.4% during the same period (*7*). Moreover, generation plus reported curtailment, indicating maximum achievable output, remained unchanged (26.5% in 2013 vs. 26.1% in 2023). This stagnation does not align with pre-2013 expectations and the sector's substantial progress over a decade.

We hypothesize that this discrepancy partially reflects "soft curtailment": unrealized wind generation that could technically be produced but is not reported in official curtailment statistics. Following the announcement of the Clean Energy Consumption Action Plan, which targeted a 5% curtailment rate (*9*), reporting practices may have become more conservative. Other operational, institutional, and market aspects may also cause reported curtailment to diverge from the broader physical definition of unused but available power. For example, generation constrained by market bidding or interconnection agreements are excluded from official statistics (*10*). Beyond potential biases in curtailment reporting, feed-in tariff deadlines have incentivized rushed installations (*11*) and potentially premature reporting of grid connection, which can distort assessments of actual operational capacity. These factors, together with the lack of systematic post-2013 assessments, motivate a long-term analysis of China's wind power underperformance.

Here we provide one of the most comprehensive evaluations of China's wind power development to date. We assemble a dataset of 10,032 wind farms commissioned between 1989 and 2022, along with their exact locations, hub heights and turbine models. Using hourly resolved simulations driven by multiple meteorological datasets, we estimate technically usable wind generation after accounting for localized wind speed and air-density variation, turbine performance degradation, and operational losses. We then compare these estimates with actual generation at both national and provincial levels, decomposing the gap into grid-connection delays, reported curtailment, and the remainder, defined as soft curtailment. Leveraging their spatiotemporal distribution of these components, we further examine how provincial energy-mix, economic and power-demand are associated with wind power underperformance. Lastly, we

evaluate the potential for economically exploit unrealized but available wind generation through storage at multiple timescales and service to emerging flexible loads, and assess the implications for China's carbon-neutrality pathways.

Results

China's Wind Power Development from Lagging to Leading

China's grid-connected wind power capacity grew from less than 1 GW when the Renewable Energy Law took effect in 2006 to over 640 GW by 2025 (*1*). Early deployment was concentrated in northern China, particularly Inner Mongolia (Fig. 1a). Nationwide feed-in tariffs introduced in 2009 supported further expansion. During the 11th Five-Year Plan (2006-2010), installed capacity increased more than 30-fold, and development subsequently began to spread beyond the traditional northern bases.

Although the 12th Five-Year Plan continued to prioritize the "Three Norths" (North, Northwest, and Northeast China), new installations increasingly expanded in central, southern, and coastal provinces after 2015. Offshore wind deployment accelerated after 2016, exceeding 30 GW by 2022 and reaching 44 GW by 2025, led primarily by Jiangsu and Guangdong. Despite this spatial diversification, northern regions still dominate cumulative installations (Fig. 1b), notably coinciding with power systems dominated by coal-fired (including combined heat and power, CHP) plants that may constrain wind power utilization.

In parallel with spatial expansion, turbine technology and domestic manufacturing capability advanced substantially under sustained policy support. A domestic content requirement (>70%) introduced in 2006 accelerated the development of local turbine manufacturing. By 2022, Chinese manufacturers accounted for approximately 64% of the global wind turbine market (*12*).

These industrial advances were accompanied by marked improvements in turbine design and scale (Fig. 1c). The average hub height of newly installed onshore turbines increased from 58 m in 2005 (below the US average of 76 m) to 111 m in 2022, surpassing the US average of 100 m that same year. Average rotor diameter increased from 55 to 171 m, while per-turbine capacities rose from 0.9 to 4.6 MW (Supplementary Table S1). In addition, turbine specific area (defined as the ratio of rotor swept area to nameplate capacity, an inverse measure of specific power) largely increased over time. This trend partially reversed after 2020, when increases in generator capacity began to outpace rotor expansion, reflecting an industry-wide shift from maximizing CFs toward minimizing costs (*13, 14*).

Importantly, these technological advances were achieved despite a gradual shift toward lower-resource sites. Long-term mean 100-m wind speeds at newly commissioned wind farms declined from 7.8 m/s for projects commissioned during 2001-2010 to 7.1 m/s during 2015-2022. Taller turbines largely offset this decline, with hub-height wind speeds decreasing only marginally from 7.3 to 7.0 m/s (Supplementary Fig. S1). Overall, the technological improvements would still be expected to improve wind energy capture. However, the performance lagged expectations. Realized CFs showed little improvement, and wind generation remained lower than that in the United States until 2016 despite surpassing it in installed capacity by 2011 (Supplementary Fig. S2). We therefore examine how changes in wind resources and turbine technology translated into theoretical and realized generation.

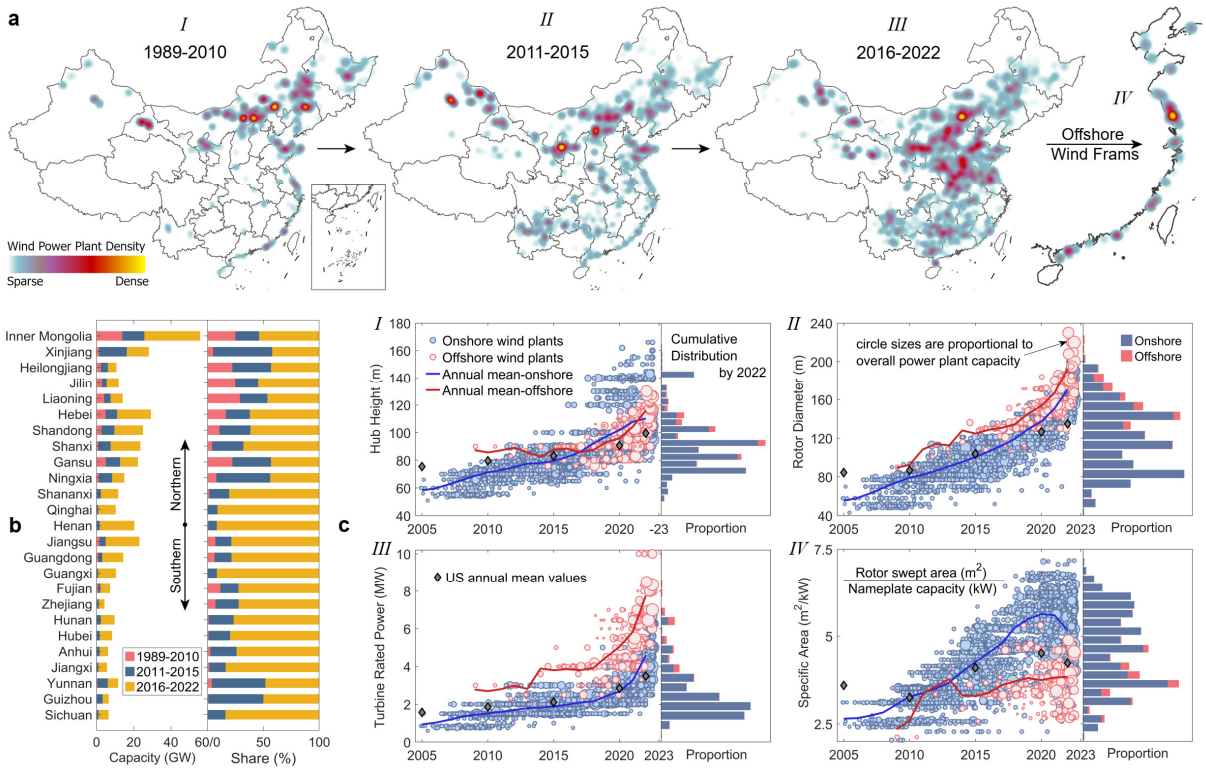


Fig. 1 Evolving wind power deployment in China. a, Heat map of wind power plant density from 1989 to 2022, with offshore wind farms displayed separately on the far right. **b**, Changes in installed capacity by province, showing only provinces with over 1 GW of capacity by the end of 2022. Yellow, blue, and red bars represent installations from 1989-2010, 2011-2015, and 2016-2022, respectively. **c**, Evolution of wind turbine attributes across onshore and offshore wind farms. Each circle represents a wind power plant, with size proportional to plant capacity. Red and blue lines indicate annual weighted averages for attribute changes, with US values shown for comparison (diamond markers). Specific area is defined within c.(IV). Right-hand bars depict attribute distribution for all installations up to 2022.

National Gaps Between Theoretical and Realized Wind Power Generation

To compare theoretical wind output to that realized in practice, we first define two metrics, both rooted in official statistics. The first is installation CF, calculated using total installed capacity, adjusted by calendar-based installation date correction (see Methods). The second is grid CF, derived from reported utilization hours for grid-connected capacity. Their difference reflects delays in grid connection (*8*). The theoretical CF (TCF) is estimated using turbine installation data from 1989 to 2022 and high-resolution (3 km) meteorological data from the China Meteorological Administration (CMA) (*15*). The estimation incorporates site-specific wind speeds and air density over time, and accounts for first-year commissioning losses and age-related turbine degradation to avoid overestimating generation (see Methods and Extended Data Fig. 1 for details).

As Fig. 2a shows, the TCF increased from about 33% before 2010 to 42% after 2020, whereas the grid CF rose only slightly, from 23% to 25%, over the same period. After wind curtailment began to be officially reported in 2010, the sum of grid CF and reported curtailment exhibited no corresponding increase for more than a decade. Thus, even after accounting for reported curtailment, realized generation increasingly diverged from theoretical generation.

We quantify this divergence using the overall reduction coefficient (ORC), defined as the ratio of grid CF plus reported curtailment to TCF (Fig. 2b). ORC is used to translate theoretical potential into technically usable generation by deducting aggregate losses (*16*). With reported curtailment accounted for in the numerator, and turbine degradation, commissioning loss, on-offshore farm availability and resource variation incorporated into TCF, ORC would be expected to remain relatively stable. This expectation is supported by the U.S. benchmark in Fig. 2b, where its ORC remains nearly constant. However, China's ORC declined persistently, implying growing losses over time beyond those already accounted for. This pattern is robust across results derived from CMA dataset, as well as from global reanalysis ones including MERRA2 (*17*) and ERA5 (*18*).

To interpret this divergence, we regard a share of wind generation losses in China as inherent to farm operation and remains stable over time, consistent with the U.S. benchmark. We estimate this fixed-loss component from the average ORC during the reference period (see Methods). After accounting for fixed losses, we define the remaining shortfall beyond reported curtailment as inferred "soft curtailment": unrealized generation that is technically achievable but not recorded as official curtailment. Accordingly, the mismatch between technical and realized wind generation - termed "generation gap" - is made up of three components: grid-connection delays, reported curtailment, and soft curtailment. Notably, the rise of soft curtailment coincides with declines in both grid-connection delays and reported curtailment, indicating a categorical redistribution rather than a comparable reduction in overall generation gap (Figs. 2c and 2d).

Grid-connection delays declined as installed capacity expanded and the share awaiting connection fell. Notable connection spikes occurred in 2015 and 2020 (Fig. 2e), when projects risked reduced or cancelled feed-in tariffs (FiT) unless grid connection was reported before year-end deadlines (key policies listed in Supplementary Table S2). By the end of 2020, 97% of cumulative installed capacity had been reported as grid-connected. More than 47 GW were reported as connected in December alone, accounting for 66% of annual additions (Fig. 2f). The year-end surges contributed to the lowest connection delays in the subsequent year (2016 and 2021).

However, the generation gap remained elevated around these surges, suggesting that some projects may have been reported as grid-connected to secure subsidies before becoming fully operational (*19*). Generation during 2015-2016 and 2020-2021 fell short of expectations, resulting in higher soft curtailment (Fig. 2c). As these projects gradually became fully functional over the following years, soft curtailment declined correspondingly (notably in 2017 and 2022). This pattern is robust to alternative assumptions regarding losses and degradation rates (Supplementary Fig. S3). Provincial records in which cumulative grid-connected capacity exceeded installed capacity in 2020 provide further evidence of reporting inconsistencies (Supplementary Table S3). Although data disruptions during the COVID-19 period may explain part of the discrepancy, the results are consistent with premature reporting of grid-connection.

Reported curtailment exceeded 15% in 2012 and 2016, prompting the launch of the Clean Energy Consumption Action Plan in 2018, targeting a curtailment rate below 5% (*9*). Since then, reported curtailment has remained near 3-4%. This decline, however, coincided with an increase in inferred soft curtailment. Under policy pressure, curtailment reporting may have become more conservative, shifting some unrealized generation outside official statistics.

Other operational and market mechanisms further contribute to soft curtailment. For example, penalties for wind power forecast errors and high ancillary-service cost allocation can incentivize operators to underreport available generation. Wind generation bore 44% of China's ancillary-

service costs in 2024 - double the share of coal and triple that of solar (*20*) - potentially encouraging more conservative day-ahead forecasts and market bids. Meanwhile, medium- and long-term contracts for coal-fired generation continue to dominant China's power markets. Renewable power, as a marginal source in the short-term market, may face very low or negative prices that discourage full utilization (*21*). Importantly, output reductions arising from market bidding (*10*), or occurring in regions where wind utilization already exceeds 95% (*9*), are excluded from official curtailment.

The absolute magnitude of soft curtailment may not be estimated precisely, as it is inferred from multiple interacting contributors that cannot yet be isolated. Nevertheless, the persistent decline in ORC (Fig. 2b) provides robust evidence of growing losses that have progressively offset technological improvements and limited corresponding gains in wind generation.

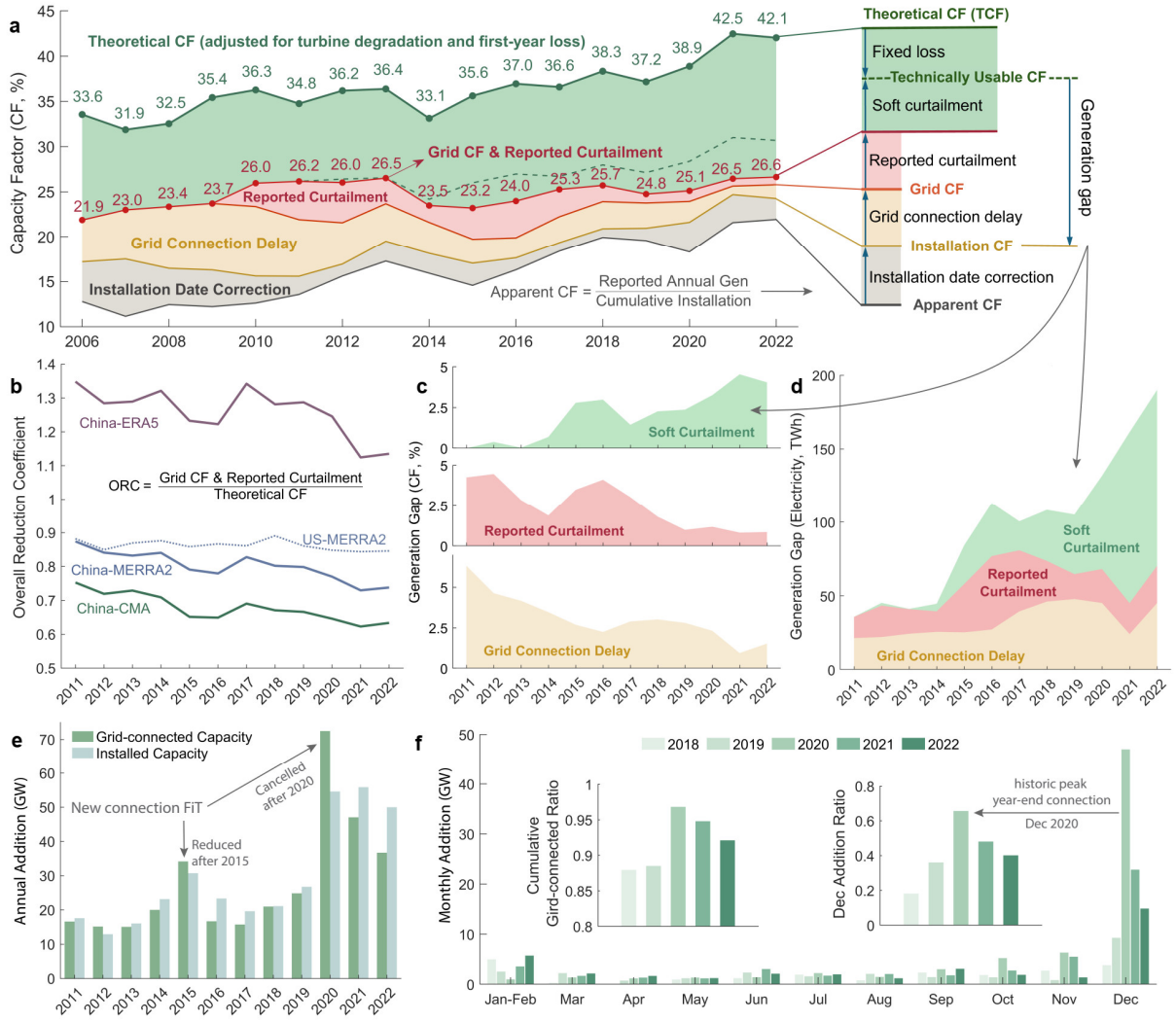


Fig. 2 The increasing gap between theoretical and realized wind power generation in China. a, National wind power capacity factors (CFs) from 2006 to 2022. Legend to the right illustrates the relation between different CF terms. **b**, The overall reduction coefficient (ORC), calculated using meteorological inputs from the China Meteorological Administration (CMA), MERRA2, and ERA5. The dashed line shows the corresponding U.S. benchmark based on MERRA2. **c-d**, Components of the

national generation gap expressed in CF (**c**) and in electricity (**d**). **e**, Annual wind power installed and grid-connected capacity additions. **f**, Monthly grid-connected wind capacity additions for 2018-2022, with insets showing the share of cumulatively installed capacity that had been grid-connected by the end of each year and the ratio of annual grid-connected capacity added in December.

Regional Heterogeneity of China's Wind Power Underperformance

To examine regional differences in wind power underperformance, we aggregate farm-level theoretical generation to the provincial level and compare it with realized generation. As shown in Figs. 3a-c, theoretical estimates are highly sensitive to meteorological inputs. Relative to results based on high-resolution data from the China's 3km data (CMA), widely used global reanalysis datasets (MERRA2 and ERA5) substantially underestimate wind potential in southern, central, and southwestern China, by roughly 40-80%. This north-south spatial bias in theoretical assessments can influence regional planning priorities and distort performance comparisons.

Among all provinces, Fujian in southeast China has the highest theoretical CF, at 51%. Its (realized) grid CF of 31% is second only to Yunnan in the southwest (32%, Fig. 3d). In contrast, most northern provinces do not achieve comparably high CFs. Notably, Inner Mongolia, the country's largest wind power base, has a relatively modest CF despite its favorable wind resources. Much of its installed capacity consists of smaller turbines with low hub heights, which limit wind energy capture (provincial comparisons in Supplementary Table S4).

Provincial ORCs during 2011-2020 also reveal substantial variation in operational losses (Fig. 3e). It is important to note that ORCs are lower in coastal provinces. Leading offshore wind regions, such as Fujian, Jiangsu, and Guangdong, exhibit ORCs in the range of 0.5-0.6, below the national average of approximately 0.7 and other reported values across China (Supplementary Text and Table S5). This pattern implies relatively high losses associated with offshore wind deployment compared with typical onshore projects. Consistently, independent analyses have shown that wake-related losses in offshore wind farms can be considerably higher than typical levels (*22*).

We group provinces into three categories according to their ORC trajectories: (A) robust decline, (B) no significant change, and (C) high volatility (Fig. 3f; see Methods and provincial ORC trajectories in supplementary Fig.S4). As in the national analysis, declining ORCs indicate increasing operational losses and inferred soft curtailment. All three categories show ORC declines around 2015 and 2020, when FiT policy promoted rushed installation and grid connection. These trends are consistent with the premature grid-connection reporting discussed.

Aggregating provincial generation gaps reveals distinct regional patterns (Fig. 3g-h; detailed in Extended Data Fig. 2). North and Northwest China have higher levels of both reported and soft curtailment, whereas southern provinces have larger grid-connection delays, consistent with their higher shares of recent installations. Northeast and Southwest China have the smallest generation gap. Electricity shortages and earlier power market reforms may have supported wind utilization in the Northeast, while abundant hydropower may provide greater operational flexibility in the Southwest. By contrast, Central China has particularly high inferred soft curtailment, driven primarily by the sustained ORC decline in Henan (Supplementary Fig. S4). Despite zero reported curtailment, Henan's grid CF fell from above 26.3% in 2011 to approximately 17.5% in 2020. The inferred soft curtailment (~6.3% CF) may extend beyond technically available but unused generation, it signals substantial operational and utilization challenges that merit examination. Given the uncertainty and inconsistencies in provincial statistics, these estimates should be interpreted primarily as indicators of relative spatial patterns rather than precise magnitudes.

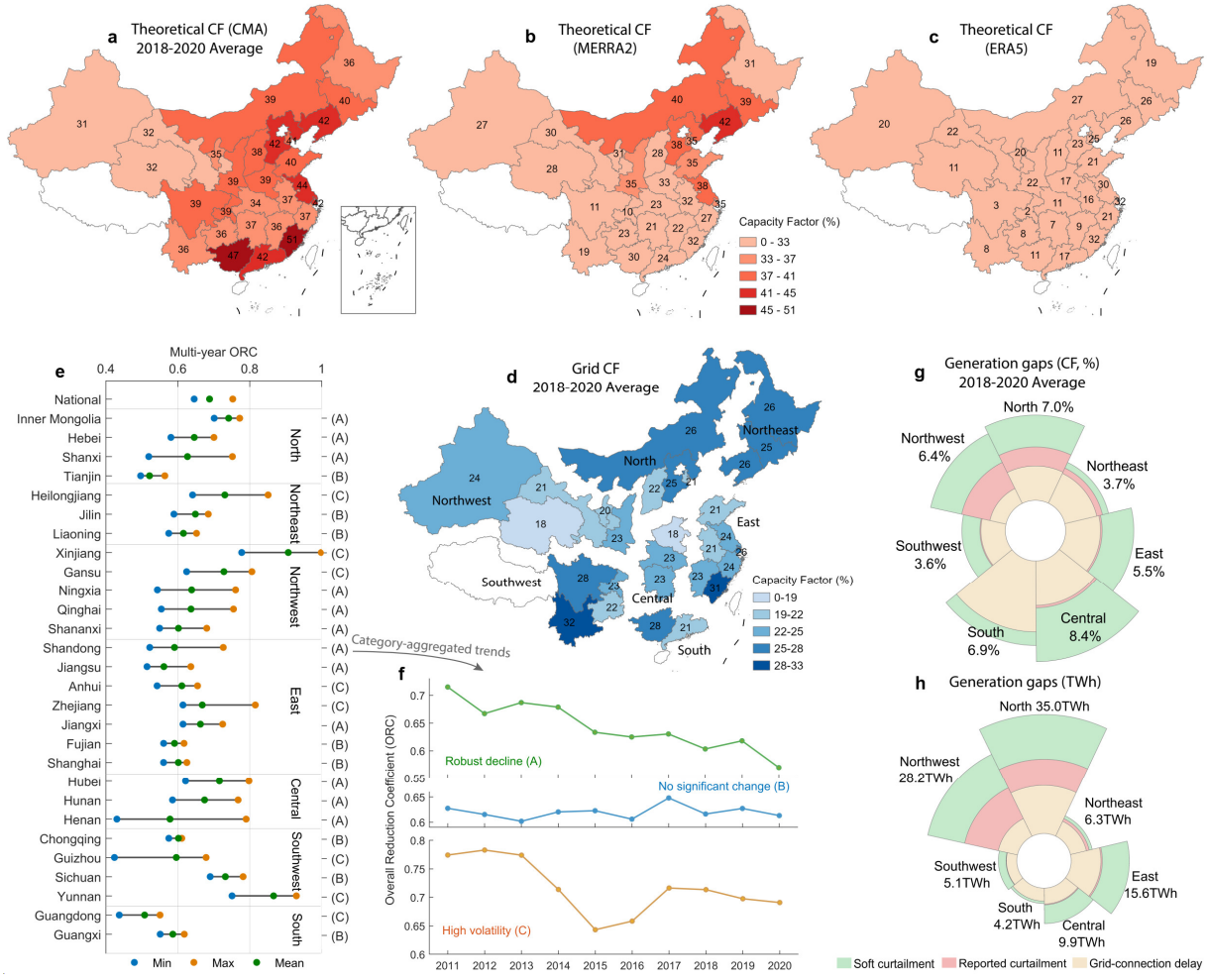


Fig. 3 Regional wind power capacity factors (CFs) and generation gaps in China. a-c, Provincial theoretical wind CFs averaged over 2018-2020, estimated using meteorological data from the China Meteorological Administration (CMA, **a**), and global reanalysis datasets MERRA2 (**b**) and ERA5 (**c**). **d**, Provincial grid CFs averaged over 2018-2020. **e**, Provincial ranges of annual overall reduction coefficients (ORCs) during 2011-2020. Provinces with year-end grid-connected capacity below 500 MW are excluded to avoid small-sample extremes. Provinces are grouped into three categories based on their ORC temporal trajectories: (A) robust decline (OLS slope < 0 and $P < 0.1$), (B) no significant trend (relative ORC variability below that of the national ORC), and (C) high volatility (relative ORC variability exceeding that of national ORC). **f**, Province-aggregated arithmetic mean ORC time series for the three trajectory categories. **g-h**, Regional generation gap, weighted by provincial realized generation, expressed as CF (**g**) and electricity generation (**h**). Provinces with year-end grid-connected capacity in the bottom quartile (~ 500 MW) are excluded to avoid small-sample extremes for CF, ORC and generation gap analysis.

Factors Shaping China's Wind Power Generation Gaps

To explore the factors associated with the generation gap documented above, we further analyze their correlations with provincial power-system characteristics. We first consider energy-mix rigidity, which constrains generation flexibility and intensifies competition among types of variable renewables; and second, we examine network and institutional rigidity, which creates connection bottlenecks and reinforcing curtailments.

Energy mix factors show different associations with reported and soft curtailment (Fig. 4a). The scale and pace of wind deployment are the most relevant. Partial correlations (see Methods) reveal that wind capacity is more strongly correlated with reported curtailment ($r = +0.57$) than with soft curtailment ($r = +0.27$). Conversely, annual wind additions are more strongly correlated with soft curtailment ($r = +0.37$) than with reported curtailment ($r = +0.19$). This distinction suggests that reported curtailment is more closely associated with the size of the existing wind fleet, whereas soft curtailment is more closely associated with recent expansion, which also reflects the FiT-driven mechanism described above.

Beyond wind deployment itself, provinces with both high CHP and high solar capacities carry the deepest reported and soft curtailment (Figs. 4a and 4b). Two compounding mechanisms may contribute to this pattern. First, in heating seasons, CHP plants must operate to meet district heating demand. This requirement creates a rigid thermal and power output that cannot be adjusted when wind and solar generation saturate the grid. Consistent with this constraint, Fig. 4c shows CHP-intensive provinces accumulating larger curtailment losses. Second, the wind-solar competition is evident in the correlations between solar capacity and wind curtailment ($r_{curt} = +0.21$, $r_{soft} = +0.36$; Fig. 4a). Solar capacity expanded 82-fold against a 4-fold increase in wind between 2011 and 2018 (Fig. 4d), and annual solar additions exceeded those of wind from 2016 to 2019 (Fig. 4e). As solar capacity approached levels comparable to wind around 2017-2018, increasing solar generation reduced the dispatch margin available to wind. Correspondingly, the correlation between solar generation and wind curtailment strengthened over time, reaching approximately +0.6 in 2018-2020 ($p < 0.01$, Fig. 4f). Reported and soft curtailment show similar patterns, although the strength of their associations differs (details in Supplementary Fig. S5).

In contrast to CHP and solar power, hydropower capacity correlated negatively with curtailment ($r_{curt} = -0.17$, $r_{soft} = -0.20$; Fig. 4a). Hydro-rich provinces also tend to have relatively low CHP heat supply, so the curtailment patterns associated with these two characteristics overlap (Figs. 4c and 4g). Seasonal complementarity between wind and hydropower may further support wind utilization. For example, in Yunnan, which has China's second-largest hydropower generation and highest wind CF, hydropower peaks during summer while wind output is strongest in winter and spring, providing natural seasonal balancing (Fig. 4h).

Network and institutional rigidity further constrain transmission flexibility. In many cases, as connection delays decline, curtailment tends to increase (Fig. 4i). Both transmission infrastructure at 220 kV+ and electricity exports are associated with smaller grid-connection delays but greater curtailment. It suggests that improved grid connection and transmission does not necessarily coincide with fuller utilization of wind generation. One possible explanation is the coupling between thermal power generation and transmission development ($r = 0.56$, Fig. 4j). This coupling is reinforced by institutional rules that tie renewable exports to thermal generation. The "wind-solar-coal bundled dispatch" mandate requires renewable exports to be paired with thermal generation (*23*), while medium- and long-term contracts further reinforce these arrangements by locking in large shares of coal-fired generation (*24-26*). A driver of this rigidity is that grid companies were obligated to uphold fixed annual operating-hours contracts with coal generators but were not required to compensate renewable producers for curtailment (*27*). These arrangements limit the scope for wind generation to displace contracted thermal output.

Demand-side conditions are also associated with regional differences in curtailment (Fig. 4i). Provinces with electricity shortages generally exhibit lower curtailment, as greater local demand absorbs more wind generation. Similarly, provinces with a larger economic share of secondary industry (Chinese parlance for non-agricultural and non-service sectors, including

manufacturing) tend to show less curtailment. This association may reflect the relatively stable electricity demand and potential flexibility of industrial loads can help accommodate wind generation.

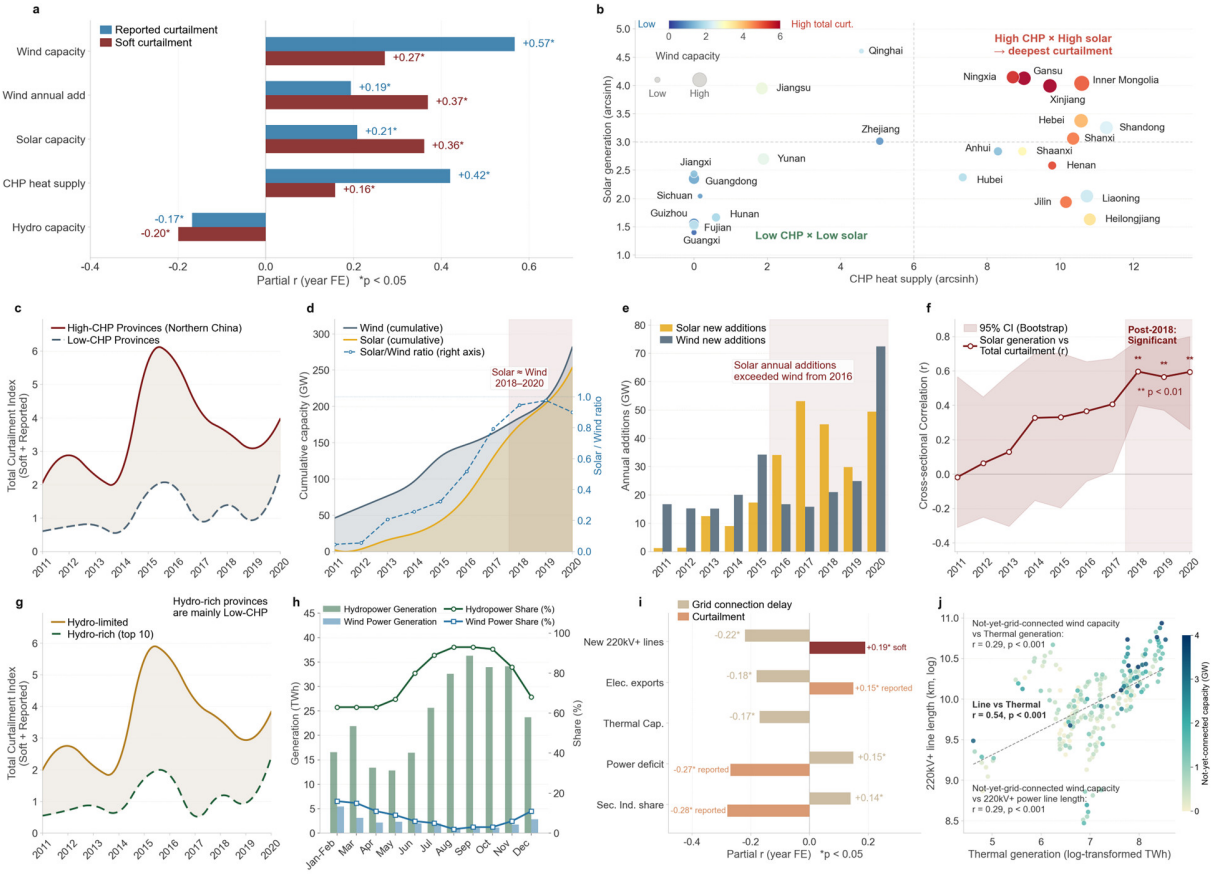


Fig. 4 Provincial associations and patterns of wind power generation gaps in China. a, Partial correlations (with year fixed effects, FE) linking predictors to reported and soft curtailment; all capacities refer to grid-connected installations. **b**, Province-level scatter of CHP heat supply against solar capacity (both arcsinh-transformed), with bubble size indicating wind capacity and color indicating weighted average wind curtailment (sum of reported and soft curtailment).**c,** Divergence in total wind curtailment between high- and low-CHP provinces. **d**, Cumulative wind and solar capacity between 2011-2020. **e**, Annual wind and solar capacity additions. **f**, Annual cross-sectional correlation coefficients (*r*) between solar generation and total wind curtailment; shaded ribbon indicates the 95% bootstrap confidence interval for the curtailment series. **g**, Divergence in total wind curtailment between hydropower-rich and hydropower-limited provinces. **h**, Monthly hydropower and wind generation in Yunnan province in 2020. **i**, Partial correlations linking predictors to grid-connection delay and wind curtailment. **j**, Scatter plots showing the association between thermal generation capacity and the length of high-voltage transmission lines (220 kV+), with not-yet-grid-connected wind capacity indicated by color.

Cost-effective Pathways to Unlock Unrealized Wind Generation

The generation gaps identified above represent an opportunity to increase wind electricity supply without installing additional turbines. These gaps amount to approximately 26.5% of realized wind generation on average during 2018-2022 (Fig.2c, d). Fully recovering this generation

would therefore provide the same electricity as an additional 26.5% of wind capacity operating at the current utilization level. We define this additional capacity as "equivalent capacity".

To access the implications for future wind deployment, we consider projected capacity trajectories under China's energy and climate goals. By the end of 2025, installed wind and solar capacities had exceeded 640 GW and 1,200 GW, respectively. China aims to increase combined wind and solar capacity to six times its 2020 level by 2035, corresponding to more than 3,600 GW in total. Based on this target, wind capacity is projected to reach approximately 1,250-1,690 GW by 2035 and further expand to 2,500-3,800 GW by 2060 under carbon-neutrality pathways (*28*). Under this assumed trajectory, full recovering the estimated generation gap could deliver the wind electricity associated with the specified 2060 capacity scenario as early as 2047, approximately 13 years earlier (expressed as equivalent capacity, Fig. 5a). Even partial recovery could accelerate this timeline, with 20-23% utilization yielding a five-year advance and 42-47% a ten-year advance (Fig. 5b).

To evaluate how much of this potential can be realized economically, we first construct hourly (8,760-h) profiles of unrealized wind power by matching provincial electricity demand with wind generation (see Methods). Their temporal patterns vary across regions (Extended Data Fig. 3a), affecting the suitability and cost of different utilization pathways. We evaluate two broad pathways. The first is direct off-grid utilization, in which unrealized wind generation is converted into energy carriers such as hydrogen or ammonia. The second is flexibility-based utilization, in which excess generation is stored and later returned to the energy system through short- and long-duration storage (e.g., batteries, fuel cells and co-firing hydrogen or ammonia in thermal plants).

Under the assessed conditions, short-duration battery storage is generally not cost-competitive with coal-based electricity. Provincial coal-based electricity prices range from 0.26 to 0.45 CNY/kWh and average ~0.36 CNY/kWh (*29*), whereas battery-based utilization costs are substantially higher (Fig. 5c). This is because the intermittent and dispersed nature of unrealized wind generation results in low battery duty-cycle. Even if only 10% of unrealized wind generation is utilized, batteries operate for only ~900 h annually, with costs rising sharply at higher utilization shares, exceeding 10.0 CNY/kWh. In contrast, long-duration storage pathways, such as power-to-hydrogen-to-power (P2H2P) systems, achieve lower costs despite round-trip efficiency losses. In those locations where low-cost geological hydrogen storage is available, P2H2P costs can fall below 0.3 CNY/kWh (Extended Data Fig. 3b), enabling economically viable utilization at scale and supporting a potential about 13-year acceleration of the 2060 wind target (Fig. 5d).

Direct use of unrealized wind generation to produce industrial energy carriers or feedstocks may offer greater economic benefits. Green hydrogen and ammonia production can become cost-competitive as early as 2025-2030. Hydrogen production costs (2-6 CNY/kg) are significantly below those of coal-based hydrogen, which can be translated into economic incentives for wind power, promoting off-grid utilization. Although both green hydrogen production and long-duration storage enable similar 2060 target-advancement timelines (~2047, Fig. 5d), the earlier economic viability of the former leads to substantially greater cumulative emissions reductions (Extended Data Fig. 3c). Under cost-effective deployment (compared to average coal-based hydrogen cost), the cumulative CO_2 reductions from utilizing unrealized wind generation can reach the equivalent of China's total emissions in 2020 by around 2045 (Fig. 5e). Given projected annual emissions of 3-7 GT CO_2/year over 2026-2060 (*30*), the cumulative reductions

of over 20 Gt CO_2 through economically viable utilization of unrealized wind generation represent a significant contribution to China's carbon-neutral transition.

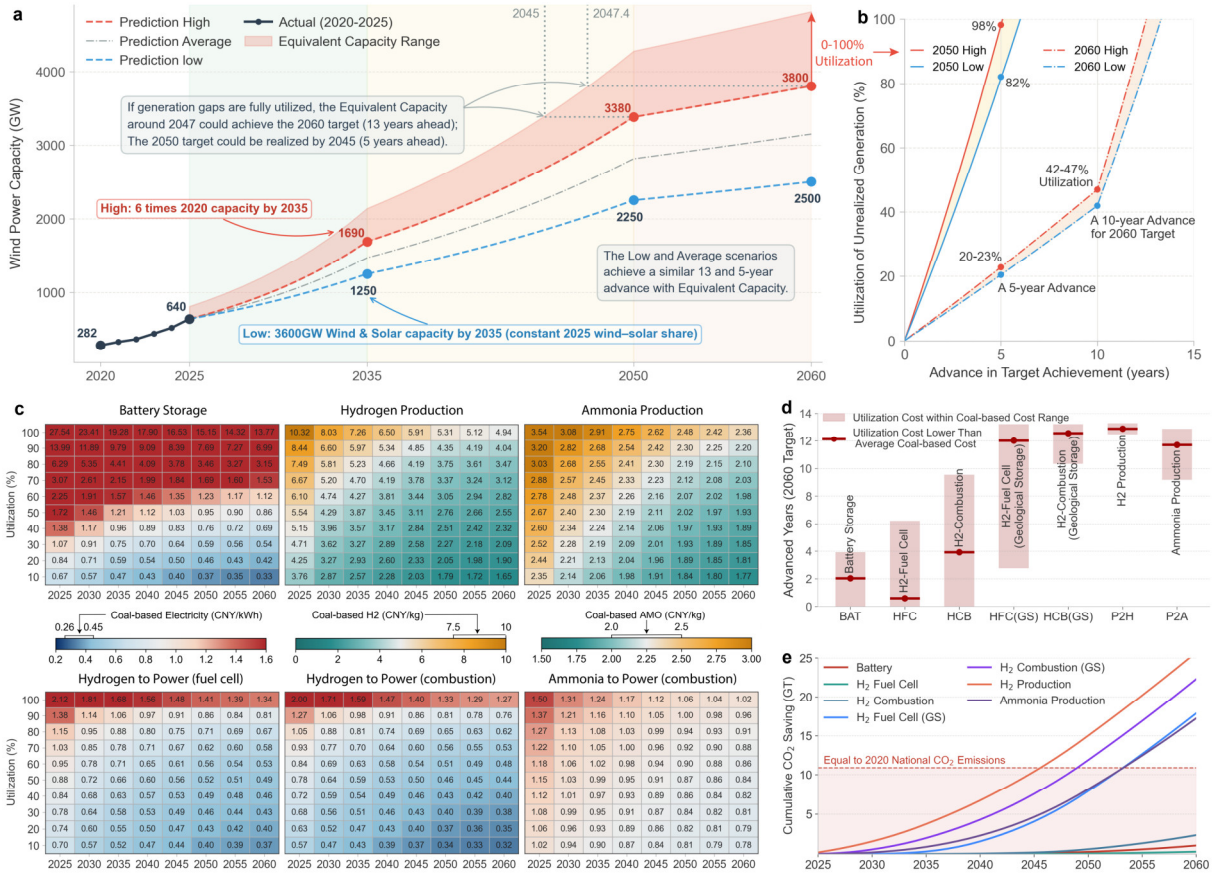


Fig. 5 Pathways and costs of utilizing unrealized wind generation in China. a, Projected wind power capacity under low, average, and high scenarios, with shaded areas indicating the equivalent capacity enabled by utilizing 100% of the generation gaps. **b**, Relationship between utilization of generation gaps and the resulting temporal advances in achieving the generation implied by the 2060 capacity target, in years. **c,** Levelized cost of electricity and chemical products for different pathways of utilization of wind generation gaps, including battery storage of electricity, production of green hydrogen and green ammonia for industrial use, and power-to-X-to-power options (fuel cells, co-fired hydrogen in gas plants or co-fired ammonia in coal plants); costs are benchmarked against costs of coal-based electricity and chemical products. **d**, Advance of the 2060 wind capacity target (average scenario) enabled by different pathways at utilization levels where costs remain below coal-based benchmarks. **e**, Cumulative CO_2 emissions reductions from utilizing unrealized wind generation across pathways at utilization levels where costs below average coal-based costs, benchmarked against China's 2020 emissions; average wind power capacity projection scenario.

Discussion and Policy Implications

Uneven Gaps Between Theoretical and Actual Wind Generation

Accurate resource assessment is fundamental to effective renewable energy planning, yet our findings reveal a persistent and spatially uneven gap between theoretical and realized wind generation that cannot be explained by meteorological uncertainty alone.

Existing national assessments commonly rely on global reanalysis datasets (*31*) together with generalized turbine specifications (*32*) and uniform loss assumptions (*33*). As shown in our results, coarse meteorological inputs can underestimate wind resources by 40-80% in southern China, while loss factors differ substantially across regions.

Future assessments should therefore combine higher-resolution meteorological datasets with empirically calibrated reference generation or correction factors. Historical observations should be updated as fleet composition and operating conditions change to refine wind generation projections. Distinguishing resource potential from technically usable and realized generation would help translate capacity targets into more realistic electricity supply projections.

Institutional Incentives Behind Generation Reporting

Administrative interventions have been effective in reducing officially reported curtailment. Following the introduction of the 5% curtailment cap in 2018 (*9*), reported curtailment fell from 12% in 2017 to an average of 3.5% during 2019-2023. This decline coincided with rising inferred soft curtailment, suggesting that changes in reporting may have contributed to the apparent improvements. After the threshold was relaxed to 10% in 2024, reported curtailment exceeded 5% again in 2025 amid continued rapid capacity expansion (*34*). These observations alone do not establish the effect of the policy change. Nevertheless, the combined grid CF and reported curtailment remained below its 2011-2013 level during 2024-2025, suggesting that the underperformance issue identified in our analysis have persisted.

The link between curtailment targets and project approvals offers one possible explanation for conservative reporting. China's renewable deployment targets are translated into provincial development plans and renewable portfolio standards. Provinces exceeding curtailment warning thresholds face restrictions on approvals for new renewable projects. Consequently, eligibility for continued capacity expansion depends on maintaining curtailment below regulatory thresholds, potentially creating incentives for conservative curtailment reporting.

Moreover, contractual and compensation arrangements may reinforce these incentives. Coal-fired generation is largely secured through medium- and long-term contracts, whereas curtailed wind and solar generation does not necessarily receive compensation. Although guaranteed renewable purchase was introduced in 2006 and strengthened in 2024 (*35, 36*), guaranteed purchase hours (GPHs, equivalent full-load hours that grid companies are required to purchase) represent only a minimum procurement obligation. By 2025, wind GPHs have declined to only 400 hours in some provinces (*37*), leaving generation beyond this minimum exposed to market risks. Excluding market-induced generation reductions from official curtailment statistics further limits the visibility of these losses.

A prerequisite for addressing these issues is greater transparency in renewable generation and curtailment reporting. Public disclosure of plant-level realized generation, together with standardized reporting of curtailment by cause (e.g., grid constraints, market participation, maintenance, and commissioning), would substantially improve the identification of utilization problems and provide a clearer basis for policy interventions.

Flexible Wind Power Utilization Beyond Subsidies

Our pathway analysis suggests that the economic value of unrealized wind generation depends on how and when it is used. Improving renewable utilization requires coordinated changes in demand, system operation, and market design. A practical near-term strategy is to shift from reactive curtailment management toward proactive demand-side utilization. Flexible electricity consumers located close to renewable resources, including hydrogen electrolyzers, data centers, and electric vehicle charging infrastructure, can absorb surplus generation locally and reduce pressure on transmission and system balancing. Compared with system-wide reforms in dispatch and grid expansion, such decentralized approaches offer a more flexible and market-oriented pathway to improve wind utilization.

Looking forward, future research should examine how coupling electricity and carbon markets can better value renewable generation, and how emerging flexibility options, such as power-to-X-to-power systems, can improve the integration of renewable and thermal generation. As renewable penetration continues to rise, realizing the full value of installed renewable capacity may become as important as expanding capacity itself for achieving carbon neutrality.

Methods

Wind Farm Information

We compiled a database of 10,032 onshore and offshore wind farms installed across China from 1989 to 2022. For each farm the database records farm name, geographic coordinates, installation year, administrative location (province and county), installed capacity, turbine model, turbine rotor diameter, hub height, per-turbine rated capacity, and an onshore-offshore classification. These attributes enable site-specific estimation of theoretical wind generation by matching each farm to local meteorological conditions and manufacturer-provided power curves.

The database covers China's cumulative installed wind capacity as of 2022, as reported by the Chinese Wind Energy Association (*38*). It records project-level installed capacity following turbine erection and commissioning inspection. Quality control included cross-referencing individual project records and aggregated capacities against multiple national and industry datasets(*39-42*), together with manually verifying turbine coordinates against Google Earth satellite imagery (see Supplementary Methods S1 for details). Provincial statistics on turbine attributes are provided in Supplementary Table S4.

Theoretical Wind Power Generation with Multiple Meteorological Datasets

Theoretical wind power generation was estimated using three meteorological datasets with different spatial resolutions: the China Meteorological Administration (CMA) dataset (~3 km) (*15*), ERA5 (~25 km) (*18*), and MERRA-2 (~50 km) (*17*). The CMA dataset, developed by the National Climate Center of the CMA, was used as the default meteorological input throughout the analysis. The global reanalysis products ERA5 and MERRA-2 were included for sensitivity analysis and cross-dataset comparison.

For the CMA dataset, wind fields were available at 10-200 m above ground level at 10 m intervals, and hub-height wind speeds and air density were obtained by vertical interpolation. ERA5 wind speeds were derived from its 137 atmospheric model levels by first converting model pressure levels to geometric heights and then applying the same interpolation procedure. For MERRA-2, hub-height wind speeds were estimated from the 10 m and 50 m wind fields using the power-law wind profile (*43*). The power-law approach was adopted because comparison against the multi-level interpolation results showed smaller estimation errors than the logarithmic wind profile. Further details of the meteorological datasets and data processing procedures are provided in Supplementary Method S2.

Theoretical wind power generation was estimated through multiple steps (see Extended Data Fig.1 for differences in estimated generation). Hub-height wind speeds were first translated into power output using manufacturer-provided power curves. The resulting generation was subsequently adjusted for air density, turbine aging degradation, first-year commissioning losses, and additional offshore operational losses. These wind-farm-specific adjustments account for systematic differences in environmental conditions and operational characteristics across national fleets. By explicitly resolving these heterogeneous losses, the remaining losses can be approximated by fixed-loss factors in the subsequent estimation of technically achievable generation.

Manufacturer-provided power curves were assigned hierarchically. For turbines with an identified model, the corresponding power curve was used directly. For turbines without an identified model but sharing the same rated capacity and rotor diameter as a known model, the average power curve of the matching turbines was assigned. For the remaining turbines, the

power curve of the known turbine type with the closest specific power (rated power divided by rotor swept area) was adopted. Following this procedure, all turbines were assigned to one of 115 representative turbine types, whose manufacturer-derived power curves (provided in the Supplementary Data) were extracted from more than 900 available turbine models. Manufacturer-provided power curves were prioritized because power-curve selection substantially affects generation estimates. Generic power curves derived from specific power (*44*) and power curves inferred from operational generation (*45*), which inherently include operational losses, can underestimate generation.

To account for air density different from the standard air density we used the method given in Millstein et al. (*44*) that adjusts hourly wind speed ($V_{h,t}$) by an air-density correction factor in equation (1).

$$V_{h,t,air} = V_{h,t} \cdot \left(\frac{\rho_{h,t}}{\rho_0}\right)^{\frac{1}{3}} \quad (1)$$

where $V_{h,t,air}$ is the air density adjusted wind speed, $\rho_{h,t}$ is the hourly air density (kg/m3) taken from meteorological datasets, and ρ_0 is the reference air density (1.225 kg/m3) used in developing power curves.

Based on the air-density-corrected hub-height wind speed, theoretical turbine output ($P_{T,t}$) and capacity factor (CF_T) was calculated using the assigned power curve and wind-farm-specific loss adjustments:

$$P_{T,t} = f(V_{h,t,air}) \cdot (1 - L_{first}) \cdot (1 - L_{deg}) \cdot (1 - L_{off}) \quad (2)$$

$$CF_T = \frac{\sum_{t=1}^{8760} P_{T,t}}{8760 \cdot Cap_{ins}} \quad (3)$$

where $f(\cdot)$denotes the power curve assigned to the wind farm; the three loss terms L_{first}, L_{deg}, and L_{off} represent first-year commissioning loss, age-related turbine degradation, and additional offshore loss, respectively; Cap_{ins} is the installed capacity of the wind farm. Provincial and national capacity factors were calculated by summing theoretical generation across wind farms and dividing by the corresponding total installed capacity, equivalent to an installed-capacity-weighted average of individual wind-farm capacity factors.

First-year commissioning loss is considered because wind farms generally exhibit lower utilization during their first year of operation because of commissioning, testing, and operational ramp-up (*16*). Analysis of multi-year operating records from more than 900 wind farms showed that first-year output was approximately 8% lower than the average output during years 2-5 (*46*). We therefore applied an 8% commissioning loss in the installation year, with L_{first}=0 in subsequent years. As an alternative treatment, the commissioning loss was distributed over the first 12 months of operation according to the number of operating months falling within each calendar year (see the following section for the commissioning-date adjustment). Thus, projects commissioned partway through a year received a proportional share of the loss in the first calendar year, with the remainder applied in the following year. This treatment changed nationally aggregated annual generation estimates by less than 0.2%; we therefore retained the simpler formulation in Eq. (2). Sensitivity tests using first-year losses of 4%, 6%, 10%, and 12% are reported in Supplementary Fig. S3.

Age-related turbine degradation was represented by a linear annual degradation rate. Based on the long-term average performance declines of 0.85% (*46*), 1.08%, and 1.52% (*47*) per year

reported in three independent studies, a default degradation rate of 1.1% yr was adopted. Sensitivity analyses were further conducted using degradation rates of 0.5%, 0.9%, 1.3%, and 1.7%/yr (Supplementary Fig. S3).

Offshore wind farms were assigned an additional loss factor to account for operational characteristics that are not fully represented by the onshore fleet. Compared with onshore projects, offshore wind farms generally experience lower availability (approximately 1.5%) (*16*) and average wake losses approximately 5 percentage points higher than typical value (*22*). Accordingly, an additional offshore loss of 6.5% was applied to all offshore wind farms. This correction was introduced when identifying the lower ORCs in coastal provinces (Fig. 3e ; the correction was not applied there to preserve the original differences). Quantitative evidence on offshore-specific losses remains limited. All the corrections were applied to reduce systematic overestimation of theoretical generation in national-scale assessments but remains a limitation when evaluating individual wind farms.

Capacity Factor Metrics and Generation Gap Assessment

Capacity factor (CF) is defined as the ratio of electricity generated over a given period to the electricity that would have been generated if the installed capacity had operated continuously at its rated power over the same period. The CF metrics used in this study (summarized in Fig. 2a) are, in descending order: theoretical CF, technically usable CF, grid CF, installation CF, and apparent CF. The calculation of these metrics was based on official annual statistics published by the National Energy Administration (*41*) and the China Electric Power Yearbook (*42*).

The theoretical CF (CF_T) represents the CF estimated from meteorological conditions and turbine characteristics. It was calculated from manufacturer power curves using hub-height wind speed after accounting for additional losses in past section.

The technically usable CF (CF_U) represents the technically achievable CF after accounting for fixed operational losses from theoretical CF:

$$CF_U = CF_T \cdot (1 - L_{fixed}) \tag{4}$$

where L_{fixed} represents the remaining operational losses after the wind-farm-specific corrections described above. Its estimation is detailed in the following generation gap assessment.

The grid CF (CF_G) was calculated as annual grid-connected electricity generation (G_{grid}) divided by the time-adjusted grid-connected capacity ($Cap_{adj,grid}$). The time-adjusted capacity was obtained by applying a time-adjustment ratio (r_{time}) derived from the reported full-load hours (FHR) following Huenteler et al. (*8*), thereby accounting for partial-year operation.

$$CF_G = \frac{G_{grid}}{8760 \cdot Cap_{adj,grid}} = \frac{FHR}{8760} \tag{5}$$

$$Cap_{adj,grid} = \frac{G_{grid}}{FHR} = Cap_{grid,y-1} + \Delta Cap_{grid,y} \cdot r_{time} \tag{6}$$

$$r_{time} = \frac{\frac{G_{grid}}{FHR} - Cap_{grid,y-1}}{\Delta Cap_{grid,y}} \tag{7}$$

where $Cap_{grid,y-1}$ and $\Delta Cap_{grid,y}$ are the grid-connected capacity at the end of the previous year plus the newly connected capacity in the current year. For a small number of province-year records, inconsistencies among the reported official statistics resulted in estimated r_{time} values outside the physically meaningful range of 0-1, implying negative operating time or operation

exceeding one calendar year for newly connected capacity. In these cases, it was constrained to the physically feasible range of 0-1.

The installation CF (CF_I) was calculated using the same annual generation but referenced to the time-adjusted installed capacity ($Cap_{adj,ins}$). The time-adjusted installed capacity was calculated as the installed capacity at the end of the previous year ($Cap_{ins,y-1}$) plus the newly installed capacity ($\Delta Cap_{ins,y}$) in the current year weighted by its fraction of available time within the year.

$$CF_I = \frac{G_{grid}}{8760 \cdot Cap_{adj,ins}} \tag{8}$$

$$Cap_{adj,ins} = Cap_{ins,y-1} + \Delta Cap_{ins,y} \cdot r_{time} \tag{9}$$

where r_{time} was calculated as the fraction of the calendar year remaining after installation. For projects lacking commissioning dates and reporting only the installation year, the r_{time} estimated from Eq. (7) was adopted as an approximation. This approximation assumes that grid-connection delays are approximately uniformly distributed across projects, such that the temporal distribution of grid-connected capacity remains similar to that of installed capacity at large scale.

The apparent CF (CF_A) was calculated directly from reported annual generation and year-end installed capacity (Cap_{ins}) without commissioning-date adjustment:

$$CF_A = \frac{G_{grid}}{8760 \cdot Cap_{ins}} \tag{10}$$

The generation gap was defined as the difference between the technically usable CF and the installation CF. It was decomposed into three components: reported curtailment, soft curtailment, and grid-connection delay. Reported curtailment was obtained directly from the official statistics published by the National Energy Administration (*41*) and the National Renewable Energy Consumption Monitoring and Early Warning Center. Grid-connection delay was quantified as the difference between the installation and grid CF, following Huenteler et al. (*8*), as the two metrics are identical in the absence of grid-connection delay.

Soft curtailment was inferred as the residual between the technically usable CF and the realized grid CF after removing officially reported curtailment. It represents technically available generation that was not utilized but is not reflected in the officially reported curtailment statistics. The fixed-loss factor, used to estimate technically usable CF, was inferred from the overall reduction coefficient (ORC), defined as the ratio of grid CF plus reported curtailment to theoretical CF, termed the overall reduction coefficient (ORC). The underlying assumption is that years with the highest ORCs represent periods with negligible soft curtailment.

For the national analysis, the fixed-loss factor was estimated from the average ORC during 2011-2013. This resulted in a default fixed operational loss of 27% for the CMA dataset. This period was selected because (i) cumulative installed capacity exceeded 50 GW, reducing fluctuations associated with the early deployment stage; (ii) ORCs derived from the same meteorological dataset remained consistent between China and the United States (Fig. 2b, MERRA-2), before subsequently diverging as China's ORC declined; and (iii) ORCs estimated for 2007, 2008 and 2010 yielded comparable loss factors, supporting the robustness of the estimate. Sensitivity analyses using fixed-loss factors from 10% to 40% are presented in Supplementary Fig. S3. Although the absolute magnitude of soft curtailment varies with the assumed loss factor, its long-term increasing trend remains robust.

Provincial ORCs exhibited substantially larger variability than the national average (Fig. 3e,f), and many provinces did not show a monotonic decline. Instead of adopting a common national value, province-specific fixed-loss factors were estimated from the average of the three highest ORCs after excluding statistical outliers. Only 2011-2020 was considered because earlier provincial statistics were incomplete and installed capacities were too small, while complete provincial wind-power statistics were no longer published by the National Energy Administration after 2020. Province-year records with cumulative capacity below the lowest 25% were excluded to improve robustness. Applying the same procedure at the national level produced identical fixed-loss estimates of 27% as default. Based on the multi-year ORC trajectories, provinces were further classified into three categories (Fig.3f) using two complementary indicators: the temporal trend estimated by ordinary least squares (OLS) regression and the relative ORC variability, calculated as (max−min)/median.

A review of reported ORCs across regions and wind-farm types in China further supported the adopted fixed-loss estimates. Reported onshore ORCs ranged from 55% to 89%. The average national fixed loss was approximately 26%, consistent with our estimate. Offshore ORCs remain more uncertain, and our analysis showed larger losses estimated for coastal provinces. Details of the literature review are provided in Supplementary Text 1 and Supplementary Table S5.

Based on the estimated fixed-loss factors, soft curtailment was calculated as the non-negative residual between the technically usable and grid CF after accounting for officially reported curtailment. The soft curtailment should be interpreted as an indicator of changes in aggregate operational losses rather than an exact measure for any individual year or province. The absolute magnitude of soft curtailment may not be estimated precisely, as it is inferred from multiple interacting contributors that cannot yet be isolated.

Correlation Analysis of Factors Driving the Generation Gap

The correlation analysis was based on the province-year generation-gap components estimated using the methods described above, including reported curtailment, soft curtailment, and grid-connection delay.

Pearson correlation coefficients were calculated between these outcome variables and a range of explanatory variables, including wind capacity, annual wind additions, CHP heat supply, solar capacity, hydropower capacity, thermal power capacity, electricity exports, power deficit, transmission infrastructure (220-kV and above), and the share of secondary industry. Right-skewed explanatory variables were transformed using either the inverse hyperbolic sine (arcsinh) or the natural logarithm according to their distributional characteristics. To isolate cross-provincial variation, year fixed effects were removed by demeaning all variables within each year. Statistical significance was evaluated using two-sided t-tests with a significance threshold of $P < 0.05$.

The temporal evolution of the relationship between solar generation and wind curtailment was evaluated by calculating annual cross-sectional Pearson correlations across provinces. Uncertainty was quantified using 1,000 bootstrap resamples of province units while preserving the within-year structure.

All explanatory variables were obtained from official statistics published by the National Energy Administration (*41*) and the China Electric Power Yearbook (*42*), and the China Statistical Yearbook (*48*).

Utilization Pathway Assessment for Unrealized Wind Generation

In the assessment, we first define the concept of equivalent capacity, representing the additional installed wind capacity that would be required to produce the same amount of electricity as the identified unrealized wind generation under the current utilization level. Thus, fully utilizing the generation gap is equivalent to increasing effective wind capacity without constructing additional wind farms. Different utilization rates therefore correspond to different equivalent capacities and can be translated into advances in achieving future wind-capacity targets.

To evaluate the utilization potential, hourly (8,760-h) provincial profiles of unrealized wind generation were constructed (Supplementary Method S3). Provincial annual generation gaps estimated were converted into hourly profiles by combining hourly wind generation with provincial hourly electricity demand. The annual demand profile was first scaled and then clipped using the hourly wind-generation profile. Electricity generation exceeding the clipped demand was treated as unrealized wind generation. The demand scaling and clipping was iteratively adjusted for each province so that the constructed provincial unrealized electricity (total of the profile) exactly matched the estimated generation gap. This procedure preserves the estimated annual magnitude of unrealized generation while generating an hourly profile that captures the high intermittency and temporal variability of surplus wind generation. The resulting profile is not intended to reconstruct the actual timing of unrealized generation, but rather to provide a representative hourly input for evaluating different utilization pathways under consistent annual generation-gap constraints. The resulting monthly distributions across regions are shown in Extended Data Fig. 3a.

The resulting unrealized wind-generation profiles were subsequently evaluated under different utilization pathways. Direct utilization pathways convert surplus electricity into energy carriers such as hydrogen or ammonia. Flexibility-based pathways store unrealized electricity during surplus periods and discharge it when demand exceeds wind generation using batteries or long-duration hydrogen- and ammonia-based storage systems. For each province, year, pathway, and utilization level, the installed capacity of the corresponding technology was optimized to minimize the levelized utilization cost (Supplementary Method S3). Increasing installed utilization capacity enables a larger fraction of unrealized generation to be utilized but simultaneously lowers equipment utilization because of the highly intermittent and dispersed nature of unrealized wind generation. The utilization cost of each pathway was calculated as the annualized system cost divided by the useful output (electricity delivered or hydrogen/ammonia produced). China's techno-economic parameters for various technologies are shown in Supplementary Tables S6.

Economic feasibility was evaluated by comparing pathway costs with the corresponding coal-based benchmarks, including coal-fired electricity and coal-based hydrogen and ammonia production. Provincial results were ranked by utilization cost and aggregated according to their unrealized wind generation to derive national utilization rates (Supplementary Method S3). The economically feasible utilization rate was then converted into an equivalent capacity and used to estimate the advancement of future wind-capacity targets. Carbon-emission reductions were estimated by multiplying the utilized unrealized electricity by China's average grid emission factor (0.5942 kg CO2/kWh) (*49*). The average grid emission factor was adopted to conservatively estimate emission reductions, rather than assuming complete displacement of coal-fired generation.

References and Notes

1. Our World in Data, Wind energy capacity (2026). https://ourworldindata.org/grapher/cumulative-installed-wind-energy-capacity-gigawatts. Accessed March 1st 2026.
2. X. Lu *et al.*, Challenges faced by China compared with the US in developing wind power. *Nat. Energy* **1**, 16061 (2016).
3. J. Grafström, Less from more: China built wind power, but gained little electricity. *Questioning the Entrepreneurial State*, 219 (2022).
4. Z. Zhuo *et al.*, Cost increase in the electricity supply to achieve carbon neutrality in China. *Nat. Commun.* **13**, 3172 (2022).
5. X. Chen *et al.*, Pathway toward carbon-neutral electrical systems in China by mid-century with negative CO2 abatement costs informed by high-resolution modeling. *Joule* **5**, 2715-2741 (2021).
6. R. Barthelmie, S. C. Pryor, Potential contribution of wind energy to climate change mitigation. *Nat. Clim. Change* **4**, 684-688 (2014).
7. China Renewable Energy Engineering Institute, China Renewable Energy Development Report 2023 (2024). http://www.creei.cn/userfiles/site/5c17640916ab4961a9908fb99e4d572e.pdf.
8. J. Huenteler, T. Tang, G. Chan, L. D. Anadon, Why is China's wind power generation not living up to its potential? *Environ. Res. Lett.* **13**, 044001 (2018).
9. NDRC (2018, December 04). Clean energy consumption plan (2018-2020). National Development and Reform Commission. https://www.ndrc.gov.cn/xxgk/zcfb/ghxwj/201812/t20181204_960958.html. Accessed June 30 2025.
10. National Energy Administration (2022, April 26). Notice of the National Energy Administration on Printing and Distributing the "Administrative Measures for Monitoring and Statistics of Wind Farm Utilization Rate". http://zfxxgk.nea.gov.cn/2022-04/26/c_1310587756.htm. Accessed June 30 2025.
11. J. Li, M. S. Ho, End-year China wind power installation rush reduces electric system reliability. *Energy Econ.* **133**, 107507 (2024).
12. Global Wind Energy Council, GWEC Global Wind Report 2024 (2024). https://gwec.net/wp-content/uploads/2024/04/GWR-2024_digital-version_final-1.pdf.
13. R. Wiser *et al.*, Forecasting wind energy costs and cost drivers: the views of the world's leading experts. LBNL-1005717 (2016).
14. R. Wiser *et al.*, Land-based wind market report: 2023 edition. U.S. Department of Energy, (2023).
15. China Meteorological Administration, China National Climate Center, Big data of China's four-dimensional wind energy resources (2018). http://www.ncc-cma.net/channel/news/newsid/10708. Accessed November 1st 2024.
16. National Energy Administration. Methods of Selecting Energy Prediction Loss Factors Value of Wind Turbines. NB/T 10992-2022 (2022).
17. R. Gelaro *et al.*, The modern-era retrospective analysis for research and applications, version 2 (MERRA-2). *J. Clim.* **30**, 5419-5454 (2017).
18. H. Hersbach *et al.*, The ERA5 global reanalysis. *Q. J. R. Meteorolog. Soc.* **146**, 1999-2049 (2020).

19. J. Yao, China Energy News, Three enterprises were punished for providing false full-capacity grid connection times (2022). https://paper.people.com.cn/zgnyb/html/2022-09/19/content_25940937.htm. Accessed December 15th 2025.
20. National Energy Administration, China Electricity Market Development Report 2024 (2025). https://www.nea.gov.cn/20250717/54ae0fdb11f04b39a5b670999c04ef81/c.html.
21. S. Zhang, J. Zhang, China's overuse of coal is causing negative power prices (2025). https://dialogue.earth/en/energy/chinas-overuse-of-coal-is-causing-negative-power-prices/. Accessed December 15th 2025.
22. S. Xu *et al.*, Substantially lower estimates in China's offshore wind potential using farm-scale spatial modeling and wake effects. *Nat. Commun.* **17**, 2043 (2026).
23. NDRC (2021, February 25). Guiding Opinions of the National Development and Reform Commission and National Energy Administration on Advancing the Integration of Power Source-Grid-Load-Storage and Multi-Energy Complementary Development. National Development and Reform Commission. https://www.gov.cn/zhengce/zhengceku/2021-03/06/content_5590895.html. Accessed June 30 2025.
24. NDRC (2022, December 2). Notice of the National Development and Reform Commission and the National Energy Administration on Ensuring the Proper Signing and Fulfillment of Medium-to-Long-Term Electricity Contracts for 2023. National Development and Reform Commission. https://www.gov.cn/zhengce/zhengceku/2022-12/23/content_5733220.html. Accessed June 30 2025.
25. E. McDonald, C. Paillard, J. Warichet, J. Zheng, Meeting power system flexibility needs in China by 2030: a market-based policy toolkit for the 15th Five-Year Plan. International Energy Agency (2024).
26. M. R. Davidson, M. M. Pearson, Static Electricity: Institutional and Ideational Barriers to China's Market Reforms. *Studies in Comparative International Development* **57**, 385-409 (2022).
27. M. Davidson, *Technology Integration in China's Electricity System: Central Targets and Local Challenges*. (2019), Policy, Regulation and Innovation in China's Electricity and Telecom Industries, pp. 134-176.
28. Technology Outlook on Wind and Solar Power toward China's Carbon Neutrality Goal (2024). https://www.icon.tsinghua.edu.cn/en/info/1068/1062.htm.
29. NDRC (2015, December 30). Notice on Reducing On-Grid Tariffs for Coal-Fired Power Generation and Electricity Prices for General Industrial and Commercial Use. National Development and Reform Commission. https://www.ndrc.gov.cn/xxgk/zcfb/tz/201512/t20151230_963541.html. Accessed June 30 2025.
30. B. Chen *et al.*, Challenges to achieve carbon neutrality of China by 2060: status and perspectives. *Sci. Bull.* **67**, 2030-2035 (2022).
31. Y. Wang *et al.*, Accelerating the energy transition towards photovoltaic and wind in China. *Nature* **619**, 761-767 (2023).
32. Z. Zhu, D. Zhang, X. Zhang, X. Zhang, Integrated modeling for the transition pathway of China's power system. *Energy Environ. Sci.* **18**, 3699-3717 (2025).
33. M. A. Giovanniello, A. N. Cybulsky, T. Schittekatte, D. S. Mallapragada, The influence of additionality and time-matching requirements on the emissions from grid-connected hydrogen production. *Nat. Energy* **9**, 197-207 (2024).
34. National Energy Administration (2024, March 28). Notice on Ensuring Renewable Energy Absorption to Guarantee High-Quality Renewable Energy Development. https://zfxxgk.nea.gov.cn/2024-05/28/c_1310777105.htm. Accessed June 30 2025.

35. NDRC (2016, March 28). Renewable Electricity Full Purchase Guarantee Management Measures. National Development and Reform Commission. http://www.nea.gov.cn/2016-03/28/c_135230445.htm. Accessed June 30 2025.
36. NDRC (2024, March 18). Measures for the Supervision of Full Guaranteed Purchase of Renewable Electricity. National Development and Reform Commission. https://www.ndrc.gov.cn/xxgk/zcfb/fzggwl/202403/t20240315_1364966.html. Accessed June 30 2025.
37. Sina Finance, Guaranteed Purchase Continues Its "Major Slide" — Who Will Safeguard Wind and Solar Returns? (2025). https://finance.sina.com.cn/stock/relnews/cn/2025-01-20/doc-inefrnxv9449806.shtml. Accessed June 30 2025.
38. China Wind Energy Association (CWEA), China Wind Power Installation Capacity Statistics Briefing (2025). https://www.cweea.com.cn/xwdt/html/39900.html. Accessed June 30 2025.
39. The Wind Power: Wind Energy Market Intelligence. https://www.thewindpower.net. Accessed June 30 2025.
40. Global Energy Monitor, Global Wind Power Tracker. https://globalenergymonitor.org/projects/global-wind-power-tracker/. Accessed June 30 2025.
41. National Energy Administration, 2019 Wind Power Grid-Connection Operation Status (2020). http://www.nea.gov.cn/2020-02/28/c_138827910.htm. Accessed June 30 2025.
42. China Electricity Council, *China Electric Power Statistical Yearbook 2022*. (China Statistics Press, Beijing, 2022).
43. C. L. Archer, M. Z. Jacobson, Evaluation of global wind power. *Journal of Geophysical Research: Atmospheres* **110**, (2005).
44. D. Millstein, S. Jeong, A. Ancell, R. Wiser, A database of hourly wind speed and modeled generation for US wind plants based on three meteorological models. *Sci. Data* **10**, 883 (2023).
45. A. C. Todd *et al.*, An independent analysis of bias sources and variability in wind plant pre-construction energy yield estimation methods. *Wind Energy* **25**, 1775-1790 (2022).
46. S. D. Hamilton, D. Millstein, M. Bolinger, R. Wiser, S. Jeong, How does wind project performance change with age in the United States? *Joule* **4**, 1004-1020 (2020).
47. I. Staffell, R. Green, How does wind farm performance decline with age? *Renewable Energy* **66**, 775-786 (2014).
48. National Bureau of Statistics of China, *China Statistical Yearbook 2022*. China Statistics Press, Beijing (2022).
49. Ministry of Ecology and Environment; National Bureau of Statistics, Announcement on the 2021 Electricity CO2 Emission Factors (No. 12 of 2024) (2024). https://www.mee.gov.cn/xxgk2018/xxgk/xxgk01/202404/W020240412827267102800.pdf. Accessed June 30 2025.

Acknowledgments: This work was supported by Sze Family Foundation, National Natural Science Foundation of China (2301291) and National Social Sciences Funding of China (23CGL057).

Author contributions:

Conceptualization: H.L., Z.W C.X., M.B.M...

Methodology: H.L., Z.W., H.J., Y.W., C.X.

Investigation: H.L., Z.W., H.J., C.X., Q.S., J.C.

Visualization: H.L., Z.W., H.J., Y.W., C.X.

Funding acquisition: C.P.N., M.B.M., C.X., Z.W.

Supervision: H.L., M.B.M.

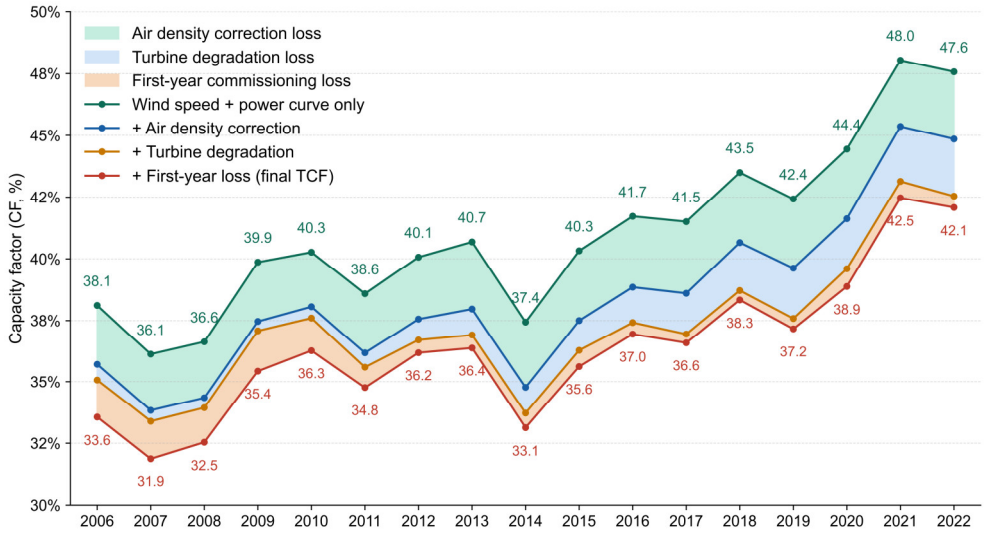
Writing – original draft: H.L., Z.W., C.X.

Writing – review & editing: H.L., Q.S., J.C., C.P.N., C.X., M.B.M.

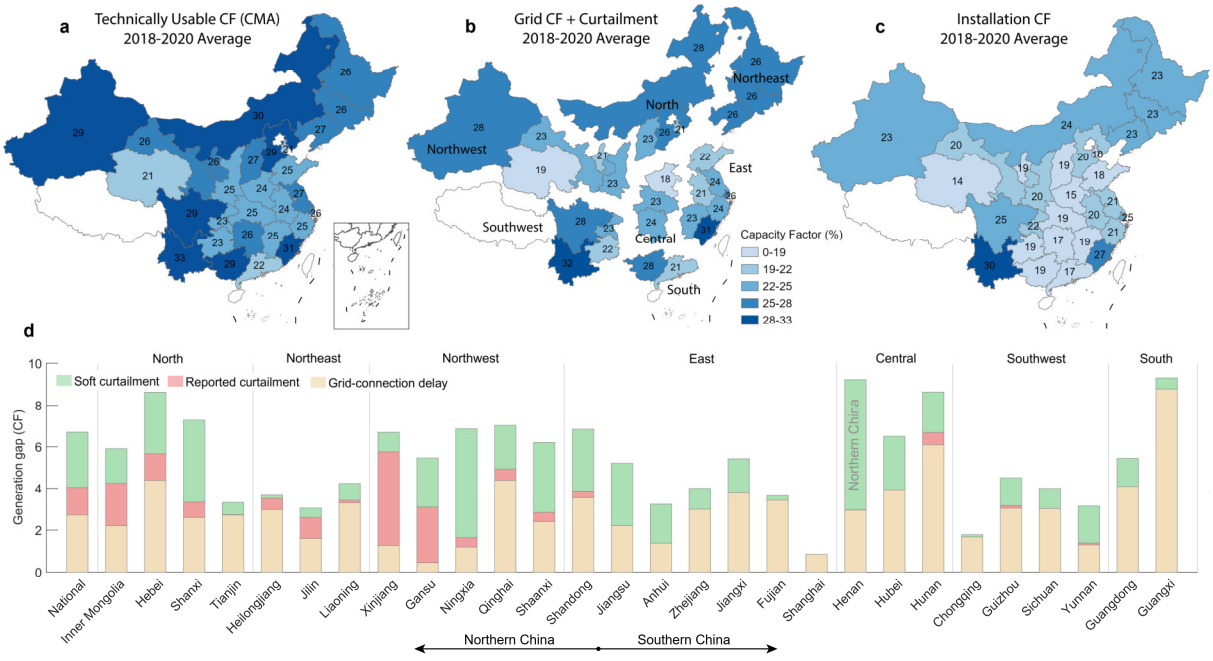
Competing interests: Authors declare that they have no competing interests.

Data and materials availability: The high-resolution wind energy resource data were developed and maintained by the National Climate Center of CMA; access for research purposes may be requested through institutional data-sharing arrangements (contact: ncc@cma.gov.cn). The wind farm database was compiled from records maintained by CMA and CWEA. Owing to data-use restrictions, the farm-level database is not publicly available; however, provincial-level aggregated statistics and the source data for the figures are provided in the Supplementary Materials. Requests for farm-level access should be directed to the corresponding authors and are subject to approval by the data providers. All other data supporting the findings of this study are available in the main text or the Supplementary Materials, with public data sources listed in the Methods and Supplementary Materials.

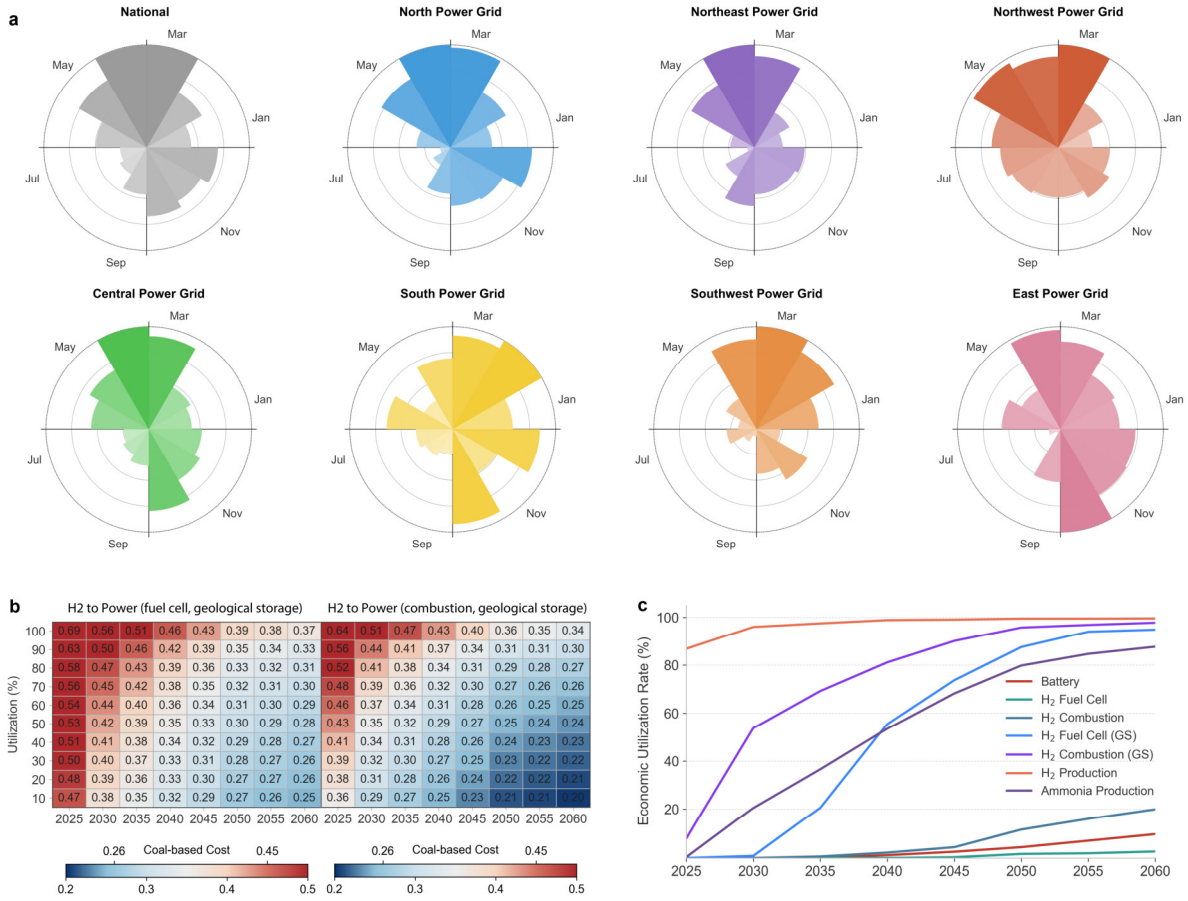
Extended data figures and tables



Extended Data Fig. 1 Stepwise decomposition of the theoretical capacity factor (TCF), 2006-2022. The dark green line shows the theoretical capacity factor calculated from turbine-specific power curves and site wind speed alone, with no further corrections. Each subsequent line and shaded band shows the cumulative effect of adding one additional correction, in order: air density correction (blue line; green shaded band), turbine age-related degradation (amber line; blue shaded band), and first-year commissioning loss (dark red line; amber shaded band). The dark red line therefore represents the fully adjusted theoretical capacity factor (TCF) used in the main text (Fig. 2a). The additional offshore operational loss is also included for offshore wind farms in final TCF but is not shown separately because its effect on the national average is negligible. These losses vary year to year with the fleet's changing siting, scale and age composition, so they are calculated explicitly for each year rather than approximated as fixed losses. This ensures the downward trend in overall reduction coefficient (ORC) in the main text reflects other relatively stable losses. Values are national annual averages across all turbines installed by each year, computed from 3-km meteorological data and turbine installation records for 1989-2022.



Extended Data Fig. 2 Provincial wind power capacity factors (CFs) and generation gap decomposition in China. a-c, Provincial averages of wind CFs over 2018-2020. The technically usable CF in (**a**) is estimated using high-resolution China Meteorological Administration (CMA) data and province-specific fixed overall reduction coefficient (ORC) for each province. Panel **b** shows grid-reported CF plus officially reported curtailment, and panel **c** shows installation-based CF accounting for commissioning timing effects. **d**, Decomposition of average provincial generation gaps (expressed in CF, %) over 2018-2020 into grid-connection delays, reported curtailment, and soft curtailment. Provinces are ordered geographically from northern to southern; Henan is administratively classified as part of Central China and therefore grouped accordingly despite its northern location.



Extended Data Fig. 3 Temporal patterns and utilization pathways of unrealized wind generation in China. a, Monthly distribution of unrealized wind generation at the national level and across regional power grids. **b,** Levelized cost of electricity for power-to-hydrogen-to-power pathways (fuel cell and hydrogen combustion in gas plants with geological storage) under different utilization levels and years, benchmarked against coal-based electricity costs. **c,** Evolution of economic utilization rates for different pathways defined as utilization levels with costs below the average coal-based benchmark.

Supplementary Materials

Supplementary Methods S1-3

Supplementary Text S1

Figs. S1 to S6

Tables S1 to S6

References (*1-54*)

Data S1

Supplementary Files

This is a list of supplementary files associated with this preprint. Click to download.

- SupplementaryData.xlsx
- Supplementary.pdf